Study of the effect of surface wettability on droplet impact on spherical surfaces

Xiaohua Liu[1,*], Kaimin Wang[1], Yaqin Fang[1], R. J. Goldstein[2] and Shengqiang Shen[1]
[1]*Key Laboratory of Ocean Energy Utilization and Energy Conservation of Ministry of Education, School of Energy and Power Engineering, Dalian University of Technology, 116024, Dalian, China;* [2]*Department of Mechanical Engineering, University of Minnesota, MN 55455, Minneapolis, USA*

Abstract

The effect of surface wettability on droplet impact on spherical surfaces is studied with the CLSVOF method. When the impact velocity is constant, with the increase in the contact angle (CA), the maximum spreading factor and time needed to reach the maximum spreading factor (t_{max}) both decrease; the liquid film is more prone to breakup and rebound. When CA is constant, with the impact velocity increasing, the maximum spreading factor increases while t_{max} decreases. With the curvature ratio increasing, the maximum spreading factor increases when CA is between 30 and 150°, while it decreases when CA ranges from 0 to 30°.

Keywords: droplet impact; surface wettability; spreading factor; impact velocity; curvature ratio

*Corresponding author: lxh723@dlut.edu.cn

Received 06 September 2019; revised 23 November 2019; editorial decision 10 December 2019; accepted 10 December 2019

1 INTRODUCTION

Droplet impact on a solid surface or liquid film occurs frequently in nature or industrial fields [1–4]. Droplet impact phenomenon can be observed in the following practical applications. During the cooling process inside a spray cooling tower, water droplets impact onto heated tubes. In a trickle bed reactor, when gas and liquid droplets flow downward, the droplets impact with the catalyst. In pharmaceutical manufacturing, solid particles are brought into a reactor and impact with liquid. In an IC engine, petrol or diesel fuel is injected onto a piston crown. Typical applications are also found in the evaporators of the multi-effect distillation seawater desalination system. The seawater droplets impact outside the surface of a horizontal tube during film evaporation.

In 1876, Worthington [5, 6] firstly conducted experiments to observe the phenomena of droplet impacting a horizontal smoked plate. Since then, driven by the interests of the phenomena and the importance of the phenomena in numerous industrial applications, researches on droplet impact were investigated all the time. Kannan *et al.* [7] experimentally explored the droplet impact behavior on a hydrophobic grooved surface. The result indicates that a trough structure changes the shape of liquid film spreading, and enhancing hydrophobicity of groove surface would be more conducive to droplet rebound. Shen *et al.* [8, 9] did a numerical simulation of the deformation process after droplet impacting a flat surface. The results show that with the decrease in the contact angle, the droplet spreading factor increases, and the oscillation frequency of droplet slows down, reaching equilibrium sooner. The volume-of-fluid (VOF) method was applied to explore the droplet spreading process with different wettability on an inclined surface. Under the same conditions, a non-wetting surface results in partial crushing of droplet. Li *et al.* [10, 11] experimentally studied the droplet impact process with different temperatures (50–120°C) and wettability. Results indicate that on part of hydrophobic surfaces, the droplet retract height increases with surface temperature, while on hydrophilic and super-hydrophobic surfaces, this rule disappears. The dynamic characteristics of droplet were also studied when impacting the surface where wettability had radial and axial symmetry gradient distribution. Quan *et al.* [12] first used a pseudopotential model of the lattice Boltzmann method and proved that retract speed and rebound tendency both increase with a better wettability. Antonini *et al.* [13] experimentally studied surface wettability effects on the characteristics of water droplet impact. When Weber number is between 30 and 200, wettability affects both droplet maximum spreading distance and spreading characteristic

International Journal of Low-Carbon Technologies 2020, 15, 414–420

doi:10.1093/ijlct/ctz077 Advance Access publication 20 January 2020

time. When Weber number is higher than 200, wettability effect is secondary because of the increase in inertial force. The VOF method was used by Liang *et al.* [14] to simulate the individual droplet dynamic behavior when droplets impact different wettability surfaces with different impact velocities. Calculation results show that a more hydrophobic surface leads to droplet rebound. The maximum spreading factor increases with the decrease in the contact angle, and the time needed to reach the maximum spreading factor reduces accordingly. The dynamic characteristics of droplet impact on curved surfaces are different from those on flat surfaces. Experimental and theoretical investigations of the impact of a droplet onto spherical target were conducted by Bakshi *et al.* [15] during which spatial and temporal variation of film thickness on the target surface was measured. When the target size is increased with respect to the droplet size, the film thinning process is slower with a larger value of residual thickness. Mitra *et al.* [16] completed a theoretical and experimental study on the effect of a spherical surface with high thermal conductivity on the super-cooled droplet impact process. Liang et al. [17] observed the phenomenon of liquid drop impact on wetted spherical surfaces at low impact velocity, using a high-speed camera. Experimental observations showed that the drop rebound and partial rebound phenomena may occur at large viscosity and low impact velocity, which cannot be observed at small viscosity. Wang [18] studied the effect of the contact angle on the droplet impact on dry spherical surfaces by the coupled level set and volume of fluid (CLSVOF) method. It was shown that the increase in the contact angle hinders droplet spreading but promotes retracting [19]. The liquid film oscillates when the contact angle is relatively small. The oscillation period decreases with increasing contact angle, while it increases with the increment in the impact velocity [20]. Zhang *et al.* [21] used the two-dimensional lattice Boltzmann model with multi-relaxation time (MRT) to simulate the liquid droplet impact on a curved target. The effects of the Reynolds number, the Weber number and the Galilei number on the flow dynamics were investigated. Zheng *et al.* [22] explored the mechanism of droplet impact on a spherical concave surface by the CLSVOF method. It was found that droplet impact on a spherical concave surface showed a smaller spread factor, earlier time of central normal jet and larger jet velocity than the impact on a flat surface. Liang *et al.* [23] experimentally investigated the heptane drop impact dynamics on wetted spheres, using a high-speed camera. The result indicates that the sphere-drop curvature ratio can greatly influence the splashing thresholds. Collision of a droplet onto a still spherical particle was experimentally investigated by Banitabaei *et al.* [24] during which the effect of wettability on collision was studied. It was found that for droplet impact onto a hydrophilic particle, the droplet is neither disintegrated nor stretched enough to form a liquid film after impact in the entire velocity range studied. However, on a hydrophobic particle, when Weber number achieves about 200 or larger, a liquid film forms after impact. With the Weber number increasing, the lamella length and cone angle increase accordingly. Another main conclusion is that increasing the contact angle from the hydrophilic to hydrophobic zone has a considerable effect on geometry of the liquid film and lamella formation. However, when the contact angle exceeds a threshold value of 110°, the increase in the contact angle has little effect on lamella geometry. A similar lamella formed after droplet impacting a small disk was observed by Rozhkov *et al.* [25] with a high-speed photography technique. Numerical researches concerning various outcomes during single liquid droplet impact on tubular surfaces with different hydrophobicity values were carried out by Liu *et al.* [19] by the CLSVOF method. When the impact velocity is constant, the increase in the surface hydrophobicity values is detrimental to the spread of the liquid film on tubular surfaces. The larger the surface contact angle is, the more likely the droplet rebound takes place. Chen *et al.* [26] conducted numerical studies on the successive impact of double droplets on a super-hydrophobic tube, using the CLSVOF method. The results showed that the impact model is dominated by the impact velocity: the out-of-phase impact takes place when the impact velocity ranges from 0.25 to 1.25 m/s, while the in-phase impact takes place when the impact velocity ranges from 1.44 to 2 m/s. Meanwhile, the occasion of the liquid crown is influenced by the impact velocity and curvature ratio.

In conclusion, the research on the droplet impacting process had a certain foundation. However, these researches mostly focused on flat surfaces, and furthermore, parameters, such as the impact velocity, droplet size and spherical curvature, needed to be investigated further. In this paper, a two-dimensional numerical simulation with the CLSVOF method is used to explore droplet dynamic characteristics of the impacting process on spherical surfaces. The impact velocity and curvature ratio are mainly studied when droplets impact spherical surfaces with different wettability; the degree of surface wettability is represented by the contact angle, CA.

2 PHYSICAL AND MATHEMATICAL MODEL

2.1 Physical model

As shown in Figure 1, a droplet impacts a spherical surface with a certain initial velocity, and the impact direction is parallel with the center line of droplet and sphere. The moment when the droplet contacts the sphere is considered as the zero moment, t signifies the evolution time of droplet impacting process, in milliseconds. In addition, u signifies the impact velocity, in meters per second, the ratio of the droplet falling distance to the time interval of which, in this paper, the impact velocity is the velocity when droplet collide with the surface the first time; d_0 signifies the initial diameter of droplet, mm; and D is the diameter of the solid sphere, mm. Other related parameters are defined as follows:

$$T^* = t \cdot u/d_0 \tag{1}$$

$$D^* = d/d_0 \tag{2}$$

$$H^* = h/d_0 \tag{3}$$

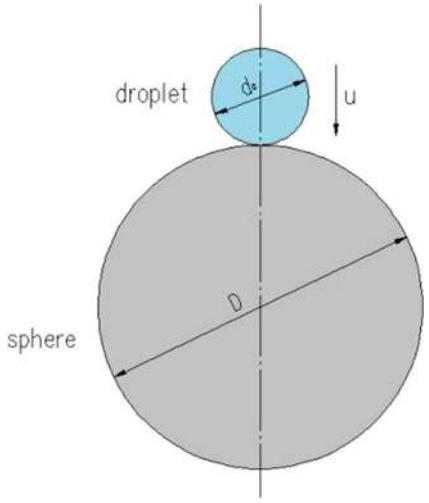

Figure 1. *A physical schematic diagram of the droplet impact on a spherical surface.*

$$\varepsilon = d_0/D \tag{4}$$

where

T^* is the dimensionless time, D^* is the spreading factor, d is the liquid film spreading diameter along the sphere, in millimeters; H^* is the dimensionless liquid film central height; h is the liquid film central height (when the liquid film rebounds into air, h represents the vertical distance from the highest point of liquid to the highest point of sphere), in millimeters; and ε is the curvature ratio.

2.2 Mathematical model

In this paper, the numerical simulations are accomplished by ANSYS Fluent 14.5 software. Droplet impacting a spherical surface is a transient process. The CLSVOF method is used by coupling VOF with level-set methods together and the advantage of which is that parameters describing phase interface with higher sharpness can be given out accurately. On the basis of mass and momentum conservation, a two-dimensional laminar axisymmetric model and Pressure-Implicit with Splitting of Operators (PISO) algorithm which has faster convergence speed are used. Liquid droplet is considered incompressible, and the calculation area is isothermal during the impact process. The droplet is water. A non-slip boundary condition is used with constant temperature, and the wall is considered smooth without roughness.

For the liquid, the control equations of mainstream field are shown as follows [27].

$$\nabla v = 0 \tag{5}$$

$$\frac{\rho \partial \boldsymbol{v}}{\partial t} + \rho \boldsymbol{v} \bullet \nabla \boldsymbol{v} = -\nabla p + \nabla \bullet \boldsymbol{v}\left[\nabla \boldsymbol{v} + (\nabla \boldsymbol{v})^T\right] - \sigma \kappa \delta(\phi) \nabla \phi + \rho g \tag{6}$$

where

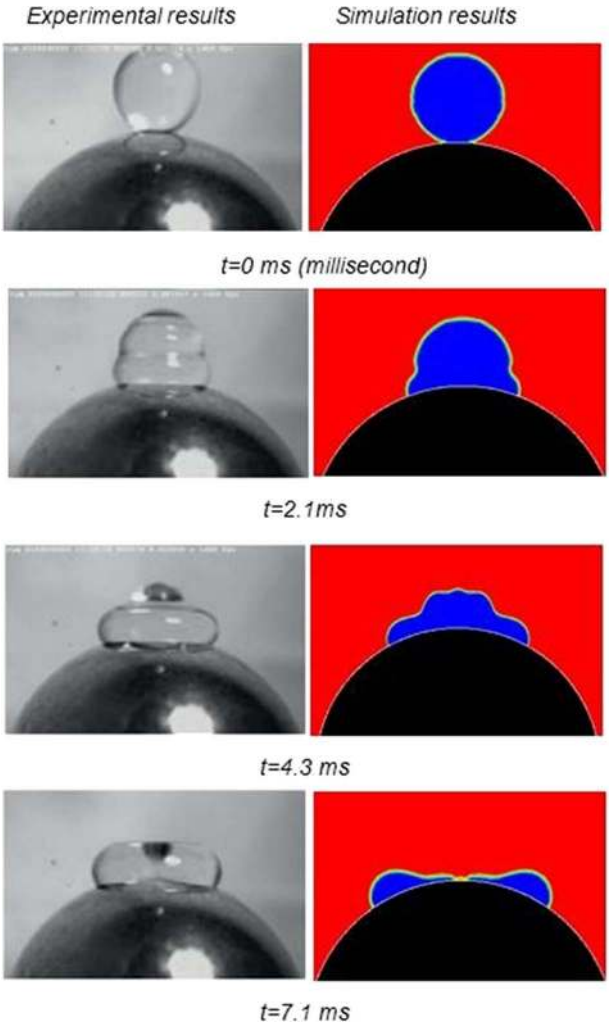

Figure 2. *The comparison of the experiment results and simulation results.*

$\boldsymbol{v}$ is the velocity vector; ρ is the density; p is the pressure; σ is the surface free energy; g is the gravitational acceleration; and κ is the interface curvature which can be calculated in Equation 7.

$$\kappa = \nabla \bullet \frac{\nabla \phi}{|\nabla \phi|} \tag{7}$$

where

$\delta(\phi)$ can be calculated with the following formula.

$$\delta(\phi) = \begin{cases} \frac{1+\cos(\pi\phi/a)}{2a} & |\phi| < a \\ 0 & |\phi| \geq a \end{cases} \tag{8}$$

where

$a = 1.5\omega$, and ω is the minimum mesh size.

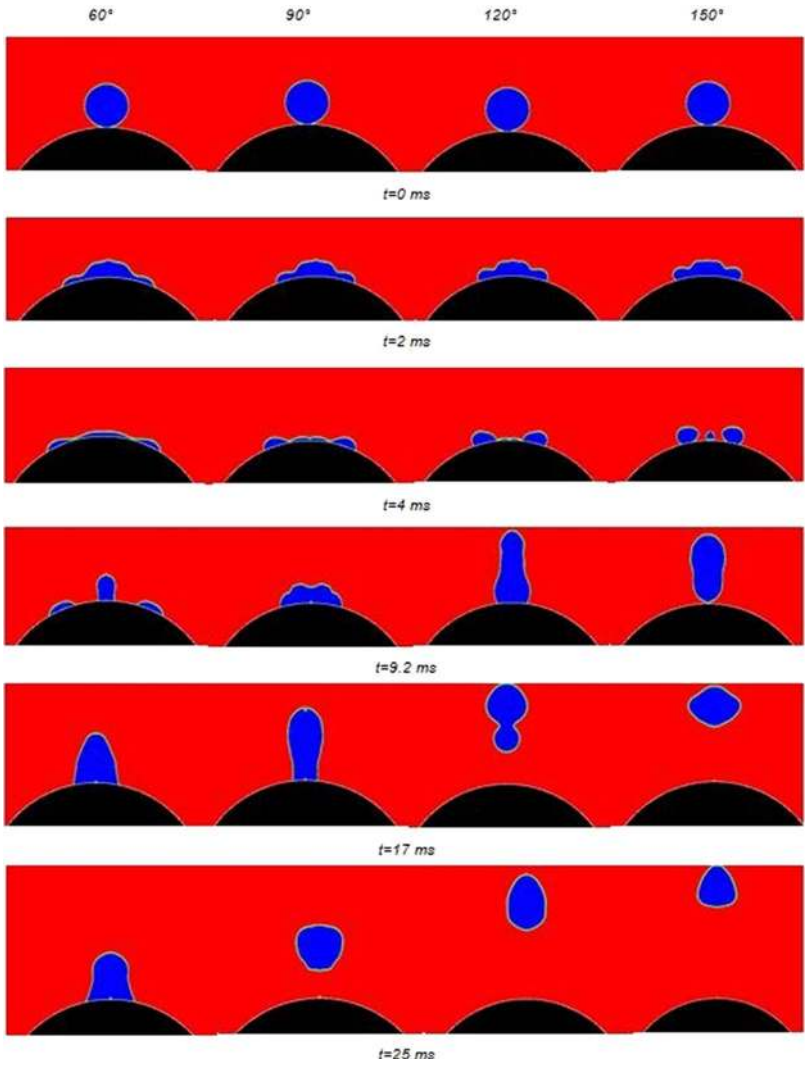

Figure 3. *Phase diagram of droplet impact on surfaces with different CA.*

3 RESULTS AND DISCUSSION

3.1 Simulation model verification

Figure 2 shows the comparison between the experimental results from Mitra *et al.* [16] and the numerical results from the simulation model used in this paper. The initial droplet diameter is 3.1 mm, the spherical diameter is 10 mm, the contact angle is 90° and the impact velocity is 0.431 m/s.

According to Figure 2, we can find that two-dimensional numerical simulation results are consistent with the experimental results at most stages of droplet impact. At the later time, there just presents a little retraction lags by two-dimensional simulation results.

3.2 Simulation results and analysis

The phase diagram of droplets impacting spherical surfaces is shown in Figure 3. The curvature ratio is 0.2, the impact velocity is 0.7 m/s and CA is 60°, 90°, 120° and 150 °, respectively. From Figure 3, the dynamic characteristics of droplet after impact are different with different contact angles. With the increment in CA, the liquid film is more prone to breakup and rebound. When CA is 90°, center sag appears at 9.2 ms. When CA is 120°, droplet complete rebounds and forms into a gourd-shape (17 ms). When CA is 150°, complete rebound takes place, and the rebound height is higher than that with CA of 120°.

The changes of the spreading factor (D^*) and the dimensionless liquid film central height (H^*) under different surface wettability are shown in Figures 4 and 5, respectively. The curvature ratio is 0.2, the impact velocity is 0.7 m/s and CA is 60°, 90°, 120° and 150°, respectively.

As shown in Figure 4, with the decrease in CA, the maximum spreading factor (D^*_{max}) and t_{max} increase. Figure 5 shows that the greater CA is, the higher the droplet rebound height and the longer the rebound time is. The main reason is that more energy remains after retraction under a larger contact angle. When CA is

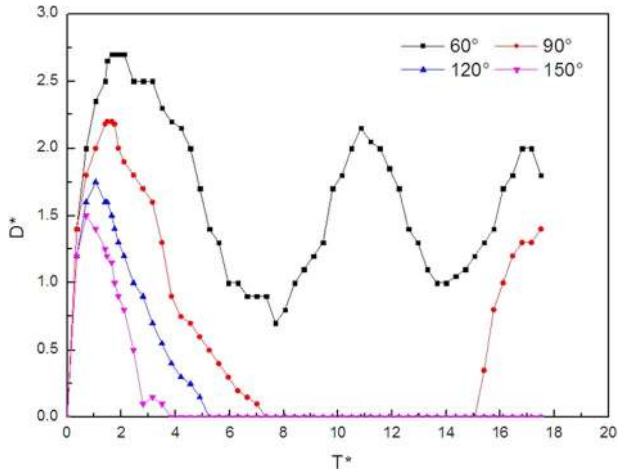

Figure 4. *The changes of D* versus T* under different contact angles.*

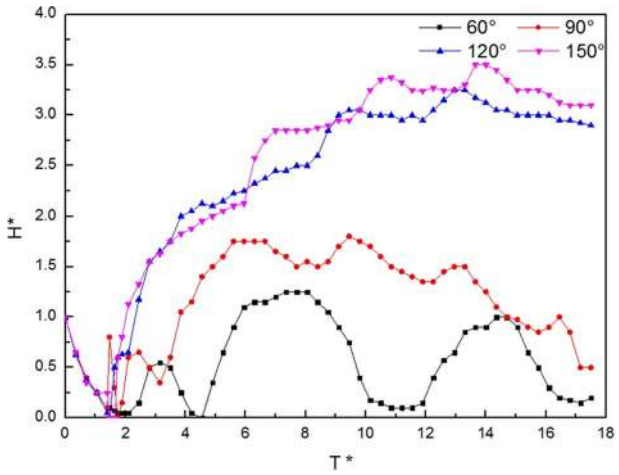

Figure 5. *The changes of H* versus T* under different contact angles*

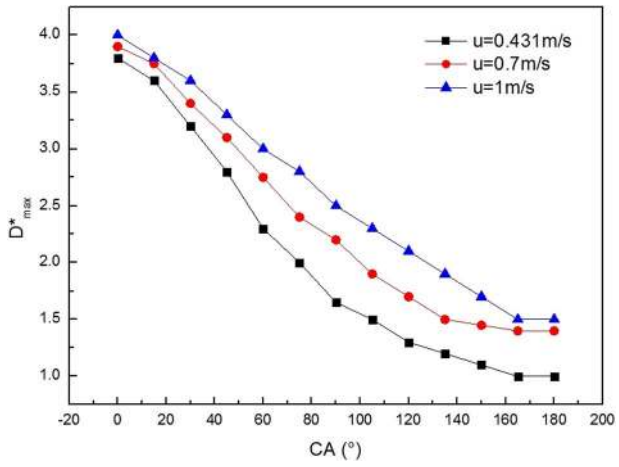

Figure 6. *Relation between CA and D^*_{max} under different impact velocities.*

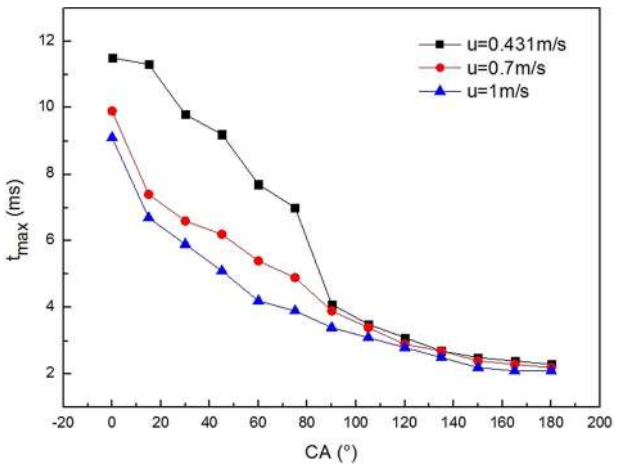

Figure 7. *Relation between CA and t_{max} under different impact velocities.*

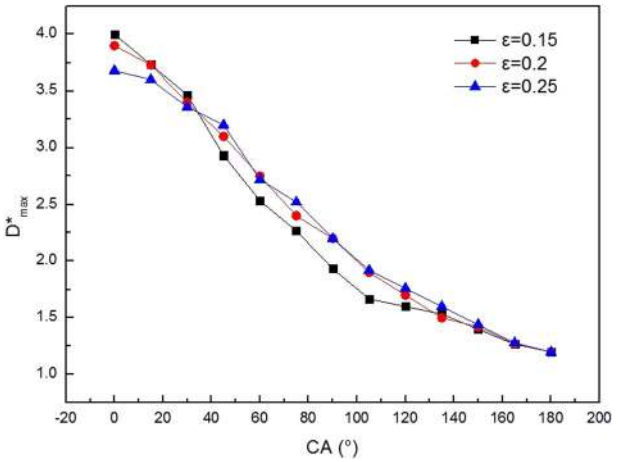

Figure 8. *Relation between CA and D^*_{max} under different curvature ratios.*

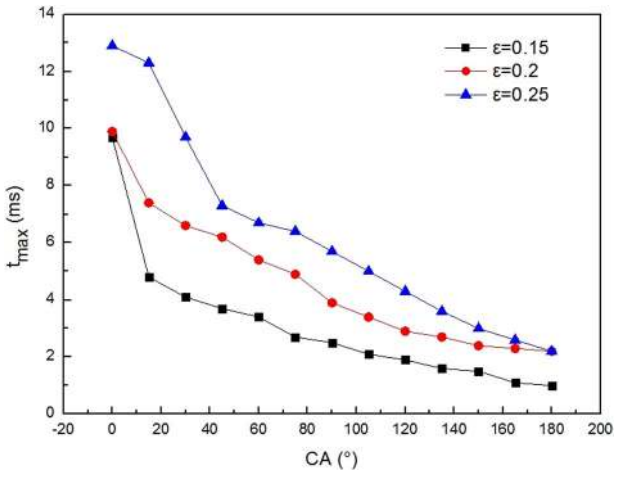

Figure 9. *Relation between CA and t_{max} under different curvature ratios.*

60°, droplet partial rebound occurs after droplet reaches D^*_{max}, the droplet retraction makes the droplet gather and then the liquid film oscillates on the surface. The spreading factor and the dimensionless film central height attenuate gradually during oscillation. When CA is 90°, the droplet also partially rebounds after droplet reaches D^*_{max}, then complete rebound happens after further retract. When CA is 120° or 150°, complete rebound occurs after spreading; the larger the contact angle is, the earlier the droplet leaves from the surface.

With different impact velocities, the relationship between CA and D^*_{max} and the relationship between CA and t_{max} are shown in Figures 6 and 7, respectively. The curvature ratio is 0.2, the impact velocities are 0.431, 0.7 and 1 m/s.

Figure 6 shows that with the decrement in CA, the maximum spreading factor becomes greater after droplet impact. This is because a better hydrophilicity is beneficial to droplet spread. For the same contact angle, the maximum spreading factor increases with the impact velocity. The reason is that the greater initial kinetic energy helps droplet to spread further. As shown in Figure 7, under the same impact velocity, the greater CA is, the smaller t_{max} is. Under the same contact angle, the lower the impact velocity is, the larger t_{max} is.

Under different curvature ratios, the relationship between CA and D^*_{max} and the relationship between CA and t_{max} are shown in Figures 8 and 9, respectively. The impact velocity is 0.7 m/s, and the curvature ratios are 0.15, 0.2 and 0.25, respectively.

As shown in Figure 8, under the same curvature ratio, the maximum spreading factor decreases with the increase in CA. The maximum spreading factor increases with the curvature ratio, when CA is between 30 and 150°. This is because the larger the curvature ratio becomes, the greater the influence of gravity on the spreading process is. When CA ranges from 0 to 30°, the maximum spreading factor decreases with increasing curvature ratio. The reason is that a better hydrophilicity promotes droplet spread and the liquid film can spread completely along the surface, and then some part liquid can even gather at the bottom of the sphere [24]. Due to high wettability of the surface and the gravity, more and more liquid would gather at the bottom of the sphere until it breaks up, during which the upper part of the sphere would expose, so the spreading factor decreases. In this case, the increment in the curvature ratio can benefit the gathering at the bottom of the sphere, which causes the upper part of the sphere to be exposed earlier and more quickly.

Figure 9 shows that under the same curvature ratio, with the increment in CA, the time needed to reach the maximum spreading factor decreases. Surface wettability affects both the maximum spreading factor and spreading characteristic time significantly [13]. Under the same contact angle, with the increment in ε, the time needed to reach the maximum spreading factor increases.

4 CONCLUSION

The effect of surface wettability on droplet dynamic characteristics after impacting is studied with the CLSVOF method. The main conclusions are as follows:

(i) With the increase in CA, the liquid film is more prone to breakup and rebound after droplet impact [19]. The rebound height and rebound time increase with CA. When complete rebound occurs, the larger CA is, the earlier the droplet rebounds away from the surface. The maximum spreading factor and time needed to reach the maximum spreading factor decrease with the increment in CA.

(ii) With the increase in the impact velocity, the maximum spreading factor increases while the time needed to reach the maximum spreading factor decreases.

(iii) The greater the curvature ratio is, the longer the time needed to reach the maximum spreading factor is. Within the range of contact angle from 30 to 150°, the bigger the curvature ratio is, the greater the maximum spreading factor is. However, within the range of the contact angle from 0 to 30°, the bigger the curvature ratio is, the smaller the maximum spreading factor is.

DISCLOSURE STATEMENT

No potential conflict of interest was reported by the authors.

ACKNOWLEDGEMENTS

This work was supported by the National Natural Science Foundation of China (No. 51476017) and Department of Mechanical Engineering, University of Minnesota.

FUNDING

Prof. Shen Xiao Wei Yang the Key Program of National Natural Science Foundation of China (NO.51936002) after (NO.51476017).

REFERENCES

[1] Rein M. Phenomena of liquid drop impact on solid and liquid surfaces. *Fluid Dyn. Res.* 1993;**12**:61–93.
[2] Josserand C, Thoroddsen ST. Drop impact on a solid surface. *Annu. Rev. Fluid Mech.* 2016;**48**:365–91.
[3] Guo YL, Wei L, Shen SQ. Simulation of dynamic characteristics of droplet impact on liquid film. *Int. J. Low-Carbon Technol.* 2014;**9**:150–6.
[4] Khojasteh D, Kazerooni NM, Marengo M. A review of liquid droplet impacting onto solid spherical particles: A physical pathway to encapsulation mechanism. *J. Ind. Eng. Chem* 2019;**71**:50–64.
[5] Worthington AM. On the forms assumed by drops of liquids falling vertically on a horizontal plate. *Proc. R. Soc. London.* 1876;**25**:261–72.
[6] Worthington AM. A second paper on the forms assumed by drops of liquids falling vertically on a horizontal plate. *Proc. R. Soc. London.* 1877;**25**:498–503.
[7] Kannan R, Sivakumar D. Drop impact process on a hydrophobic grooved surface. *Colloids Surf.* 2008;**317**:694–704.
[8] Shen SQ, Li Y, Guo YL. Numerical simulation of droplet impacting on isothermal flat solid surface. *J. Eng. Therm. Phys.* 2009;**30**:2116–8.
[9] Shen SQ, Yu H, Guo YL *et al.* Numerical simulation for splashing of single drop impact on spherical liquid film. *J. Therm. Sci. Technol.* 2013;**12**:20–4.

[10] Li XY, Ma XH, Lan Z. Behavioral patterns of drop impingement onto rigid substrates with a wide range of wettability and different surface temperatures. *AIChE J.* 2009;**55**:1983–92.
[11] Li XY, Mao LQ, Ma XH. Dynamic behavior of water droplet impact on microtextured surfaces: The effect of geometrical parameters on anisotropic wetting and the maximum spreading diameter. *Langmuir* 2013;**29**:1129–38.
[12] Quan SL, Li S, Li WZ *et al.* A simulation of impact of droplets on solid surfaces by using the lattice Boltzmann method. *Chin. J. Comput. Mech.* 2009;**26**:627–32.
[13] Antonini C, Amirfazli A, Marengo M. Drop impact and wettability: From hydrophilic to super-hydrophobic surfaces. *Phys. Fluids* 2012;**24**:102104.
[14] Liang C, Wang H, Zhu X *et al.* Numerical simulation of droplets impact on surface with different wettability. *CIESC J.* 2013;**64**:2745–51.
[15] Bakshi S, Roisman Ilia V, Tropea C. Investigations on the impact of a drop onto a small spherical target. *Phys. Fluids* 2007;**19**:032102.
[16] Mitra S, Sathe MJ, Doroodchi E *et al.* Droplet impact dynamics on a spherical particle. *Chem. Eng. Sci.* 2013;**100**:105–19.
[17] Liang GT, Guo YL, Shen SQ. Observation and analysis of drop impact on wetted spherical surfaces with low velocity. *Acta Phys. Sin.* 2013;**62**:184703.
[18] Wang YL. 2013. *Numerical study on droplet impacting spherical surfaces.* Dalian, DLUT: M.S. Thesis.
[19] Liu XH, Zhao YM, Chen S *et al.* Numerical research on the dynamic characteristics of a droplet impacting a hydrophobic tube. *Phys. Fluids* 2017;**29**:062105.
[20] Yan Z, Li Y, Li C *et al.* Numerical simulation study of droplet impact on various solid surfaces. *J. Therm. Sci. Tech.* 2018;**17**:8–14.
[21] Zhang D, Papadikis K, Gu S. Investigations on the droplet impact onto a spherical surface with a high density ratio multi-relaxation time lattice-Boltzmann model. *Commun. Comput. Phys.* 2014;**16**:892–912.
[22] Zheng ZW, Li DS, Qiu XQ *et al.* Numerical analysis of coupled level set-VOF method on droplet impact on spherical concave surface. *CIESC J.* 2015;**66**:1667–75.
[23] Liang GT, Guo YL, Mu XS *et al.* Experimental investigation of a drop impacting on wetted spheres. *Exp. Therm. Fluid Sci.* 2014;**55**:150–7.
[24] Banitabaei SA, Amirfazli A. Droplet impact onto a solid sphere: Effect of wettability and impact velocity. *Phys. Fluids* 2017;**29**:062111.
[25] Rozhkov A, Prunet-Foch B, Vignes-Adler M. Impact of water drops on small targets. *Phys. Fluids* 2002;**14**:3485–501.
[26] Chen H, Liu XH, Wang KM *et al.* Numerical study on dynamic characteristics of double droplets impacting a super-hydrophobic tube with different impact velocities. *Int. J. Comput. Fluid Dyn.* 2019;**33**:222–33.
[27] Liang GT, Shen SQ. Yang Y. CLSVOF simulation for splashing of single drop impact on flat liquid film. J. of Therm. *Sci. Technol.* 2012;**11**:8–12.